

Turing mechanism for homeostatic control of synaptic density during *C. elegans* growth

Heather A. Brooks and Paul C. Bressloff

Department of Mathematics, University of Utah 155 South 1400 East, Salt Lake City, Utah 84112, USA

(Received 16 April 2017; published 21 July 2017)

We propose a mechanism for the homeostatic control of synapses along the ventral cord of *Caenorhabditis elegans* during development, based on a form of Turing pattern formation on a growing domain. *C. elegans* is an important animal model for understanding cellular mechanisms underlying learning and memory. Our mathematical model consists of two interacting chemical species, where one is passively diffusing and the other is actively trafficked by molecular motors, which switch between forward and backward moving states (bidirectional transport). This differs significantly from the standard mechanism for Turing pattern formation based on the interaction between fast and slow diffusing species. We derive evolution equations for the chemical concentrations on a slowly growing one-dimensional domain, and use numerical simulations to demonstrate the insertion of new concentration peaks as the length increases. Taking the passive component to be the protein kinase CaMKII and the active component to be the glutamate receptor GLR-1, we interpret the concentration peaks as sites of new synapses along the length of *C. elegans*, and thus show how the density of synaptic sites can be maintained.

DOI: [10.1103/PhysRevE.96.012413](https://doi.org/10.1103/PhysRevE.96.012413)**I. INTRODUCTION**

The dynamical processes underlying the establishment of synaptic connections during neural development are thought to be critical in learning and memory. One of the most important signaling pathways underlying the maturation, maintenance, and elimination of synapses is the interplay between type II calcium- and calmodulin-dependent protein kinase (CaMKII) and the trafficking of glutamate receptors. Since these proteins are conserved across multiple species, considerable insights into synaptic development can be obtained by studying simpler organisms, such as the nematode worm *Caenorhabditis elegans*; see Fig. 1. During larval development of *C. elegans*, the density of ventral and dorsal cord synapses containing the glutamate receptor GLR-1 is maintained despite significant changes in neurite length [1]. It is known that the coupling of synapse number to neurite length requires CaMKII and voltage-gated calcium channels, and that CaMKII regulates the active (kinesin-based) transport and delivery of GLR-1 to synapses [1–3]. However, a long outstanding problem has been identifying a possible physical mechanism involving diffusing CaMKII molecules and motor-driven GLR-1 that leads to the homeostatic control of synaptic density.

Although the above problem arises within the context of neural development, it raises a more general issue regarding self-organization in systems of actively and passively transported particles. That is, (i) the formation of a regularly spaced distribution of synaptic puncta at an early stage of development is suggestive of some form of Turing-like pattern formation and (ii) the maintenance of synaptic density as the organism grows is suggestive of “pulse or stripe insertion” in spatially periodic patterns on growing domains [4]. Following the original work of Turing [5], the traditional mechanism for spontaneous pattern formation is the interaction of two or more passively diffusing chemical species undergoing nonlinear reaction kinetics and having different rates of diffusion [6–8]. Recently, motivated by issue (i), we proposed an alternative pattern-forming mechanism [9], involving the interaction between a slowly diffusing species

(e.g., CaMKII) and a rapidly advecting species (e.g., GLR-1) switching between anterograde and retrograde motor-driven transport (bidirectional transport). Using the classical Gierer and Meinhardt mechanism for reaction kinetics [10], we showed that our model supported in-phase Turing patterns on a one-dimensional domain of fixed length. Within the context of synaptogenesis in *C. elegans*, the periodically spaced concentration peaks are interpreted as the locations of synaptic puncta. (Note that Turing pattern formation based on advecting species has also been considered within the context of animal movement and chemotaxis [11].) However, in the latter case, all species are assumed to undergo bidirectional transport, and in the fast switching limit the model reduces to a traditional reaction-diffusion model for pattern formation. In our model, pattern formation cannot occur in the fast switching limit. Advection also plays a role in reaction-diffusion systems subject to active fluid flow [12].

In this paper, we address issue (ii), namely, how is the synaptic density of *C. elegans* maintained as the worm grows? From the perspective of self-organizing systems, this corresponds to the issue of whether or not the Turing mechanism based on interacting diffusing and advecting species exhibits pulse or stripe insertion on a growing domain. We establish the latter by extending the analysis of Crampin *et al.* [4] to our diffusion-advection model, and thus provide an experimentally testable explanation for the homeostatic control of synaptic density in *C. elegans*. Our main hypothesis is that synaptogenesis in *C. elegans* is an example of pattern formation on a growing domain, analogous to stripe insertion in patterns of skin pigmentation of the marine angelfish [13].

II. MODEL

The homeostatic control of synaptic density appears to be mediated by two distinct antagonistic effects of CaMKII; see Fig. 2. As the worm grows in size, the synaptic density along the ventral cord decreases, which tends to result in reduced synaptic excitation of the motor neurons. In this situation, the activation of CaMKII via voltage-gated calcium

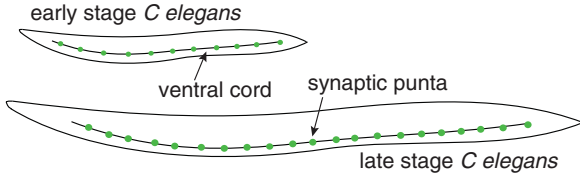


FIG. 1. Schematic figure showing distribution of synaptic puncta along ventral cord of early and late stage *C. elegans*. New synapses are inserted during development to maintain the synaptic density.

channels induces the formation of new synapses by enhancing the active transport of GLR-1. On the other hand, when the synaptic density becomes too high, the corresponding increase in excitation leads to constitutive activation of CaMKII (autophosphorylation) due to the increased calcium levels. Although constitutively active CaMKII also enhances the motor-driven transport of GLR-1 along the ventral cord, it fails to localize the receptors at synaptic sites. This is consistent with the observation that the synaptic localization of CaMKII in rate changes in response to autophosphorylation [14].

To model this system, consider a one-dimensional domain of fixed length L , which represents a neurite in the ventral cord of *C. elegans* at a particular stage of larval development. Let $R(x,t)$ denote the concentration of GLR-1 receptors at position x along the cell at time t and let $C(x,t)$ denote the corresponding concentration of active CaMKII. For simplicity, no distinction is made between membrane-bound (synaptically localized) and cytoplasmic CaMKII. On the other, GLR-1 is partitioned into two subpopulations: those that undergo anterograde transport (R_+) and those that undergo retrograde transport (R_-) with $R(x,t) = R_+(x,t) + R_-(x,t)$. Individual receptors randomly switch between the two advective states according to a two-state Markov process $R_+ \xrightleftharpoons[\alpha]{\beta} R_-$, with transi-

tion rates α, β . This yields the following system of equations [9]:

$$\frac{\partial C}{\partial t} = D \frac{\partial^2 C}{\partial x^2} + f(R_+, R_-, C), \quad (1a)$$

$$\frac{\partial R_+}{\partial t} = -v \frac{\partial R_+}{\partial x} + \alpha R_- - \beta R_+ + g(R_+, C), \quad (1b)$$

$$\frac{\partial R_-}{\partial t} = v \frac{\partial R_-}{\partial x} + \beta R_+ - \alpha R_- + g(R_-, C). \quad (1c)$$

Here D is the CaMKII diffusion coefficient and v is the speed of motor-driven GLR-1. The reaction term $f(R_+, R_-, C)$ represents both the self-activation of CaMKII and the inhibition of CaMKII by GLR-1. (In a more detailed model, one could consider synaptic rather than cytoplasmic GLR-1 inhibiting synaptic rather than cytoplasmic CaMKII.) The reaction terms $g(R_{\pm}, C)$ represents the increase in actively-transported GLR-1 due to the action of CaMKII, which is taken to be symmetric with regards anterograde and retrograde transport. Equations (1) are supplemented by reflecting boundary conditions at the ends $x = 0, L$:

$$\left. \frac{\partial C(x,t)}{\partial x} \right|_{x=0,L} = 0, \quad (2a)$$

$$v R_+(0,t) = v R_-(0,t), \quad v R_+(L,t) = v R_-(L,t). \quad (2b)$$

For simplicity, we will take $\alpha = \beta$ in the following.

It remains to specify the form of the chemical interaction functions f and g . The precise details of the interactions between CaMKII and GLR-1 are currently unknown. Therefore, we choose the simplest model that can capture the activation of GLR-1 transport and delivery by CaMKII and the inhibition (synapse removal) of CaMKII by GLR-1 and the autophosphorylation properties of CaMKII. Another requirement is that the nonlinear interactions yield Turing patterns for which the peaks of the various concentrations are in-phase. Hence, following our previous work [9], we take the classical activator-inhibitor system due to Gierer and Meinhardt (GM) [10]:

$$f(R_+, R_-, C) = \rho_1 \frac{C^2}{R_+ + R_-} - \mu_1 C + \gamma, \quad (3a)$$

$$g(R, C) = \rho_2 C^2 - \mu_2 R. \quad (3b)$$

Here ρ_1, ρ_2 represent the strength of interactions, μ_1 and μ_2 are the respective decay rates, and γ is the production rate of CaMKII. To justify the trafficking-based mechanism for pattern formation in *C. elegans*, the conditions for Turing instability must be satisfied for biophysically relevant parameters. Many of these parameters can be cited from the biological literature. First, we require $\mu_1 < \mu_2$ for stability in the homogeneous steady state in this system; this is satisfied because the decay rate of GLR-1 is approximately four times that of CaMKII [15]. For our simulations (see Sec. III), we

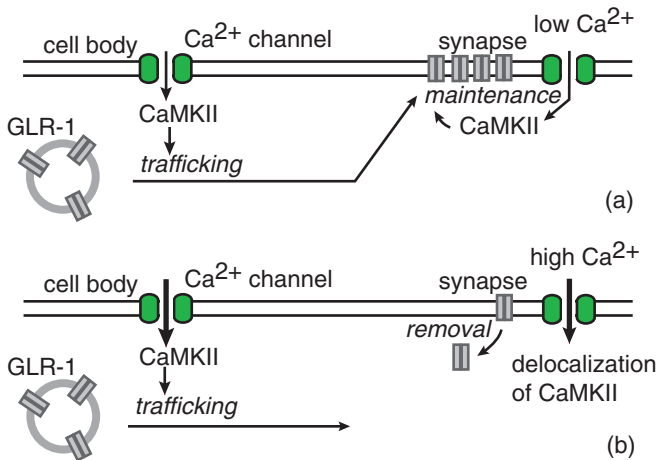


FIG. 2. Regulation of transport and delivery of GLR-1 to synapses by CaMKII. (a) Calcium influx through voltage-gated calcium channels activates CaMKII, which enhances the active transport and delivery of GLR-1 to synapses. (b) Under conditions of increased excitation, higher calcium levels results in constitutively active CaMKII which fails to localize at synapses, leading to the removal of GLR-1 from synapses.

take $\mu_1 = 0.25/s$ and $\mu_2 = 1/s$. Additionally, data on the transport of GLR-1 via molecular motors suggest an average velocity along the ventral cord is $1 \mu\text{m}/s$, with an average run length of $9.2 \mu\text{m}$ [16]. From this, we infer a switching rate of $\alpha \approx 0.11/s$. We take diffusion of CaMKII to be $0.01 \mu\text{m}^2/s$ and production rate to be $\gamma = 0.02 \mu\text{M}/s$. Finally, we set the strength of interaction parameters to be $\rho_1 = 1/s$ and $\rho_2 = 1/(\mu\text{M s})$.

III. PATTERN FORMATION ON A GROWING DOMAIN

Previously, we used linear stability analysis to derive conditions for a Turing instability, and confirmed numerically that spatially periodic patterns emerge beyond the Turing bifurcation point [9]. In particular, we found that $\gamma = \alpha D/v^2$ has to be sufficiently small for patterns to emerge. One consequence is that patterns emerge outside the parameter regime of fast switching (large α), where the linearized model reduces to a two-component reaction-diffusion system. Here we investigate pattern formation on a slowly growing 1D domain, $0 < x < L(t)$, where $L(t)$ is the increasing length of the domain. The basic idea is that $L(t)$ represents the length of *C. elegans* at a time t during development, following an initial phase of synaptogenesis at time $t = 0$. This means that the model system is already operating beyond the Turing bifurcation point identified in our previous paper [9]. If we interpret the in-phase peaks of CaMKII and GLR-1 as synaptic sites, then the wavelength of the pattern at time $t = 0$ is equivalent to the spacing of the newly formed synapses. This suggests that under uniform growth of the domain for $t > 0$, the spacing of the synapses will increase. Therefore, to obtain a similar synaptic density in the adult as in the first stages of synaptogenesis, it is necessary for new synaptic puncta to be formed. From the mathematical perspective, this can be interpreted as stripe insertion of a Turing pattern on a growing domain.

In light of the above, consider the system of advecting and diffusing particles (1) on the growing domain $0 < x < L(t)$. Following previous studies of diffusion processes on growing domains [4], we model domain growth in terms of a velocity field u such that $x \rightarrow x + u(x,t)\Delta t$ over the time interval $[t, t + \Delta t]$. We will assume spatially uniform growth by taking $\partial_x u = \sigma(t)$, which implies that

$$u(x,t) = \frac{x}{L(t)} \frac{dL(t)}{dt}. \quad (4)$$

Let $X \in [0, L_0]$ be the local coordinate system at the initial length L_0 . Using a Lagrangian description, we can then represent spatial position at time t as

$$x = \Lambda(X,t) \equiv \frac{XL(t)}{L_0}, \quad L(0) = L_0.$$

To derive the evolution equations on a growing domain, let us focus on the diffusing component $C(x,t)$; the other components can be treated in a similar fashion. Consider the particle conservation equation

$$\frac{d}{dt} \int_0^{L(t)} C(x,t) dx = \int_0^{L(t)} \left[-\frac{\partial J(x,t)}{\partial x} + f \right] dx, \quad (5)$$

with $J(x,t) = -D \frac{\partial C(x,t)}{\partial x}$. Using the Reynold's transport theorem, the left-hand side becomes

$$\begin{aligned} \frac{d}{dt} \int_0^{L(t)} C(x,t) dx \\ = \int_0^{L(t)} \left[\frac{\partial C(x,t)}{\partial t} + \frac{\dot{L}(t)}{L(t)} \frac{\partial [xC(x,t)]}{\partial x} \right] dx. \end{aligned}$$

We thus obtain the following evolution equation for C on $0 < x < L(t)$:

$$\frac{\partial C}{\partial t} + \frac{\dot{L}(t)}{L(t)} \frac{\partial [xC]}{\partial x} = D \frac{\partial^2 C}{\partial x^2} + f. \quad (6)$$

Finally, we transform Eq. (6) to the fixed interval $[0, L_0]$ by performing the change of variables $x \rightarrow X = (xL_0)/L(t)$. Under this transformation the advection term in Eq. (6) is eliminated and we obtain the modified evolution equation,

$$\frac{\partial C}{\partial t} = \frac{D}{L(t)^2} \frac{\partial^2 C}{\partial X^2} - \left(\frac{\dot{L}}{L} \right) C + f(R_+, R_-, C). \quad (7a)$$

Applying a similar analysis to the advecting variables $R_{\pm}(x,t)$, with fluxes $J_{\pm}(x,t) = \mp v R_{\pm}$ and $f(R_+, R_-, C)$ replaced by $\pm(\alpha R_- - \beta R_+) + g(R_{\pm}, C)$, we derive the following evolution equations on $[0, L_0]$:

$$\begin{aligned} \frac{\partial R_+}{\partial t} = -\frac{v}{L(t)} \frac{\partial R_+}{\partial x} - \left(\frac{\dot{L}}{L} \right) R_+ + \alpha R_- - \beta R_+ \\ + g(R_+, C) \end{aligned} \quad (7b)$$

$$\begin{aligned} \frac{\partial R_-}{\partial t} = \frac{v}{L(t)} \frac{\partial R_-}{\partial x} - \left(\frac{\dot{L}}{L} \right) R_- + \beta R_+ - \alpha R_- \\ + g(R_-, C). \end{aligned} \quad (7c)$$

In the above equations, we have fixed the length-scale by setting $L_0 = 1$.

Equations (7a)–(7c) and (3a), (3b) are the starting point for our investigation of Turing pattern formation on a growing domain of length $L(t)$. Following Ref. [4], we make one further simplification by noting that for sufficiently slow growth, the terms involving the dilution factor $-\dot{L}(t)/L(t)$ are small compared to the remaining terms and can be neglected. It is reasonable to assume slow growth for *C. elegans*, since the larvae grow to the adult stage at an average rate of around $10^{-3} \mu\text{m}/s$ [17]. For the sake of illustration, we will assume logistic growth [4],

$$L(t) = e^{rt} \left[1 + \frac{1}{\Lambda_0} (e^{rt} - 1) \right]^{-1}, \quad (8)$$

with $r = 0.001 \mu\text{m}/s$ and $\Lambda_0 = 10$. With this choice of growth function, a section of the ventral cord grows from $10 \mu\text{m}$ to $100 \mu\text{m}$ in 2 h. Although we choose this logistic growth function because it represents the physical growth during *C. elegans* development, similar results are obtained for other choices of growth functions (such as exponential or linear).

In our numerical simulations, we assume that the system of evolution equations operates beyond the Turing bifurcation point for pattern formation at the initial length L_0 . The initial concentrations are chosen from a uniform random distribution

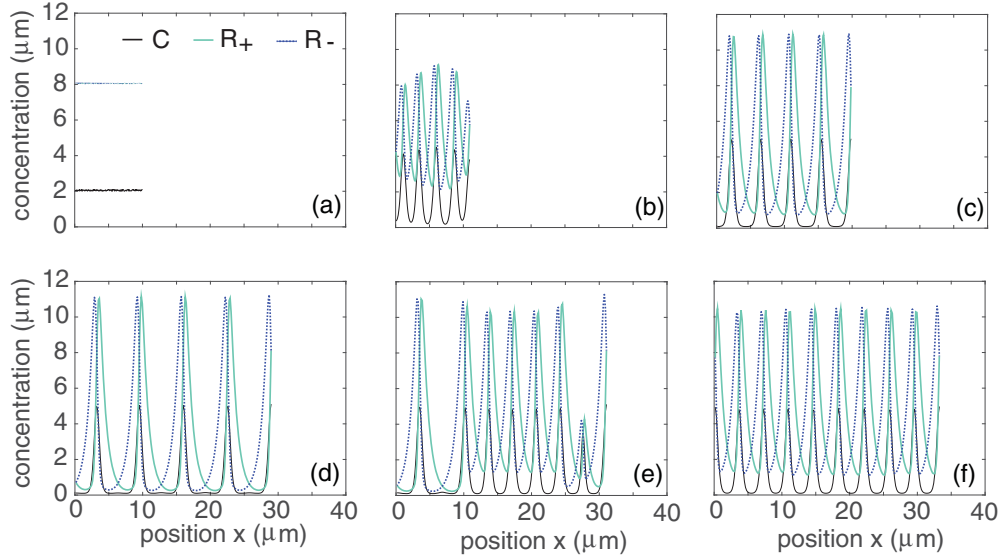


FIG. 3. Numerical simulations showing temporal evolution of the concentrations C, R_{\pm} on a slowly growing domain. (a) $t = 0$ s; (b) $t = 100$ s; (c) $t = 850$ s; (d) $t = 1300$ s; (e) $t = 1400$ s; (f) $t = 1500$ s. Initial concentrations are taken to be random fluctuations about steady-state values. A spatially periodic pattern is becoming established with five potential synapse sites by $t = 100$ s, and as the domain continues to grow, the synapse sites begin to spread out. At $t = 1300$ s, we can see the beginnings of pattern reorganization between the synapse sites as CaMKII concentrations start to grow there. New peaks are inserted after the second, third, and fourth existing synapse sites by $t = 1400$ s; the beginnings of a new CaMKII peak can also be observed between the first and second peak. Numerical simulations were performed using a combination of Crank-Nicolson and Lax-Wendroff schemes, with no flux boundary conditions. Full solutions were computed in the Lagrangian coordinate system, and then converted back into physical coordinates. We take space step $dx = 0.05$ and time step $dt = 0.025$. The 1D domain grows with growth parameters $r = 0.001 \mu\text{m/s}$ and $\Delta_0 = 10$. Other parameters are $\rho_1 = 1/\text{s}$, $\rho_2 = 1/(\mu\text{M s})$, $\mu_1 = 0.25/\text{s}$, $\mu_2 = 1/\text{s}$, $\alpha = 0.11/\text{s}$, $D = 0.01 \mu\text{m}^2/\text{s}$, $\gamma = 0.02 \mu\text{M}/\text{s}$, and $v = 1 \mu\text{m}/\text{s}$.

near fixed point values of the spatially uniform equations. Example plots showing the evolution of the concentrations C, R_{\pm} are shown in Fig. 3. As the system evolves, we initially observe growth of the concentration C of the diffusive component, and then patterns emerge as the activator is eventually tempered by increase of the advecting inhibitors R_{\pm} . In this case, the concentration of both activating and inhibiting species are in phase with each other. Once the pattern

is established, it persists as the domain length increases, with areas of high concentration slowly growing farther apart. As the areas of high concentration become sufficiently separated, the pattern becomes reorganized and we see the emergence of new peaks.

Having established that the Turing mechanism based on interacting advecting and diffusing species supports pulse-insertion on a growing domain, we can now relate our results to the particular problem of homeostatic control of synaptic density in *C. elegans*. That is, interpreting C and R_{\pm} as concentrations of CaMKII and GLR-1, respectively, we can interpret the peaks in concentration as synaptic sites. Hence, the insertion of additional peaks as the domain grows provides a mechanism for maintaining synaptic density. This is illustrated in Fig. 4, which shows a space-time plot of CaMKII and GLR-1 concentrations in a growing domain. For the given parameter values, our results match well the experimental observations of Rongo and Kaplan [1], who found that *C. elegans* synaptic density is maintained.

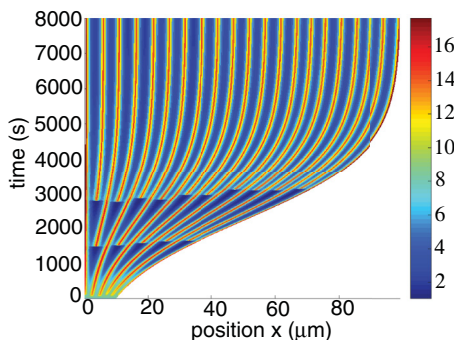


FIG. 4. Space-time plot showing the insertion of new potential synaptic sites as the domain representing a section of the ventral cord grows over the course of 2.5 h. The horizontal axis represents position along the *C. elegans* ventral cord and the vertical axis represents time in seconds. Colors represent local concentration of GLR-1 (a combined total of both leftward and rightward trafficking species) in μM . Areas of high concentration represent potential synapse sites. Numerical simulations and parameter values are as in Fig. 3.

IV. DISCUSSION

In summary, we have shown how an active trafficking-based mechanism for Turing pattern formation on a 1D growing domain can account for the homeostatic regulation of synapses in *C. elegans* during development. While the important role of CaMKII in regulating the delivery of GLR-1 to synapses along the ventral cord of *C. elegans* is well known, the detailed mechanisms regarding their interactions are still unclear. In future modeling work, it will

be necessary to develop a more detailed biophysical model of CaMKII-GLR-1 coupling, and to distinguish between membrane-bound versus cytoplasmic CaMKII. Nevertheless, our simple model can provide experimentally testable predictions, particularly with regard the spacing of synaptic puncta. For example, linear stability analysis can determine the wavelength of emerging patterns as a function of various biophysical parameters such as the diffusivity of CaMKII, the speed and switching rates of molecular motors, and the rate of CaMKII phosphorylation. Our model predicts that manipulation of these parameters should change the synaptic spacing. On the other hand, the insertion of new puncta should persist.

From the more general perspective of self-organizing systems, our model provides a new paradigm for exploring pattern-forming dynamical systems, based on nonlinear interactions between distinct advecting and diffusing species. Although our model involved molecular species, one could equally well consider population models of animal species. One obvious extension would be to analyze the generation of patterns in higher spatial dimensions. In the case of the neurites in *C. elegans*, the microtubules tend to be aligned in

parallel so that one can treat the active transport process as effectively 1D. On the other hand, intracellular transport within most non-polarized animal cells occurs along a microtubular network projecting radially from an organizing centers or centrosomes [18]. It has been found that microtubules bend due to large internal stresses, resulting in a locally disordered network, suggesting that *in vivo* transport on relatively short length scales may be similar to transport observed *in vitro*, where microtubular networks are not grown from a centrosome and thus exhibit orientational and polarity disorder [19,20]. If the network is sufficiently dense, then to a first approximation one can assume that the set of velocity states (and associated state transitions) available to an active particle is independent of position. This means that one can effectively represent active transport within the cell in terms of a two- or three-dimensional velocity jump process [21–23], which is analogous to an animal movement model with a turning function [24,25]. One of the interesting features of higher dimensional models, is that one has to use weakly nonlinear analysis to derive amplitude equations for the emerging patterns close to the Turing bifurcation point, to investigate the selection and stability of patterns (rolls, rhomboids, and hexagons).

-
- [1] C. Rongo and J. M. Kaplan, *Nature* **402**, 195 (1999).
 [2] F. J. Hoerndli, D. A. Maxfield, P. J. Brockie, J. E. Mellem, E. Jensen, R. Wang, D. M. Madsen, and A. V. Maricq, *Neuron* **80**, 1421 (2013).
 [3] F. J. Hoerndli, R. Wang, J. E. Mellem, A. Kallarackal, P. J. Brockie, C. Thacker, E. Jensen, D. M. Madsen, and A. V. Maricq, *Neuron* **86**, 457 (2015).
 [4] E. J. Crampin, E. A. Gaffney, and P. K. Maini, *Bull. Math. Biol.* **61**, 1093 (1999).
 [5] A. M. Turing, *Philos. Trans. R. Soc. B* **237**, 37 (1952).
 [6] A. J. Koch and H. Meinhardt, *Rev. Mod. Phys.* **66**, 1481 (1994).
 [7] J. D. Murray, *Mathematical Biology. II Spatial Models and Biomedical Applications*, Interdisciplinary Applied Mathematics Vol. 18 (Springer-Verlag, New York, 2001).
 [8] D. Walgraef, *Pattern Formation with Examples from Physics, Chemistry, and Materials Science* (Springer-Verlag, New York, 1997).
 [9] H. A. Brooks and P. C. Bressloff, *SIAM J. Appl. Dyn. Syst.* **15**, 1823 (2016).
 [10] A. Gierer and H. Meinhardt, *Kybernetik* **12**, 30 (1972).
 [11] T. Hillen, *J. Math. Biol.* **35**, 49 (1996).
 [12] J. S. Bois, F. Julicher, and S. W. Grill, *Phys. Rev. Lett.* **106**, 028103 (2011).
 [13] S. Kondo and R. Asai, *Nature* **376**, 765 (1995).
 [14] K. Shen and T. Meyer, *Science* **284**, 162 (1999).
 [15] C. Hanus and E. M. Schuman, *Nat. Rev. Neurosci.* **14**, 638 (2013).
 [16] M. I. Monteiro, S. Ahlawat, J. R. Kowalski, E. Malkin, S. P. Koushika, and P. Juoa, *Mol. Biol. Cell.* **23**, 3647 (2012).
 [17] J. E. Sulston and H. R. Horvitz, *Dev. Biol.* **56**, 110 (1977).
 [18] P. C. Bressloff, *Stochastic Processes in Cell Biology* (Springer, Berlin, 2014).
 [19] A. Kahana, G. Kenan, M. Feingold, M. Elbaum, and R. Granek, *Phys. Rev. E* **78**, 051912 (2008).
 [20] H. Salman, A. Abu-Arish, S. Oliel, A. Loyter, J. Klafter, R. Granek, and M. Elbaum, *Biophys. J.* **89**, 2134 (2005).
 [21] O. Bénichou, C. Loverdo, M. Moreau, and R. Voituriez, *J. Phys.: Condens. Matter* **19**, 065141 (2007).
 [22] C. Loverdo, O. Benichou, M. Moreau, and R. Voituriez, *Phys. Rev. E* **80**, 031146 (2009).
 [23] P. C. Bressloff and J. M. Newby, *Phys. Rev. E* **83**, 061139 (2011).
 [24] T. Hillen and H. G. Othmer, *SIAM J. Appl. Math.* **61**, 751 (2000).
 [25] T. Hillen and A. Swan, in *Mathematical Models and Methods for Living Systems*, edited by L. Preziosi *et al.*, (Springer, Berlin, 2016), pp. 73–129.